Thrust Force Characteristics of Propulsion Mechanism Modeled on Bending Mechanism of Eukaryotic Flagella in Water*

Shunichi KOBAYASHI**, Masaya NAKASONE**,
Kozo FURIHATA*** and Hirohisa MORIKAWA**

The application of dynamics observed in organisms is very instructive in the field of engineering. We noted the utility of eukaryotic flagellar motion for propulsion in water, and made an enlarged propulsion mechanism modeled on the active sliding of microtubules in eukaryotic flagella. Active sliding between two rows of electromagnets on flexible beams corresponding to the active sliding of microtubules was used. Cyclic two-dimensional bending movement and positive thrust force of the propulsion mechanism were generated in water. We discussed the influence of the bending frequency, the number of waves, and the sliding length on the thrust force.

Key Words: Flagella, Flagellar Motion, Microtubules, Propulsion, Biomimetics, Biomechanics, Robotics

1. Introduction

Since most organisms are fairly autonomic, functional and efficient, the study of machines modeled on the motions of organisms is very significant in the engineering field. From this point of view, we aimed at examining the micropropulsion mechanism modeled on aquatic microorganisms. As a guide for the microrobot design, we proposed a micropropulsion mechanism in water modeled on the active sliding of microtubules of eukaryotic flagella, such as spermatozoa, and conducted a computer simulation[1),(2)]. This mechanism is based on a new artificial bending propulsion mechanism hung in water which imitates the "sliding" by microtubules and their "elastic deformation". It involves a relatively simple structure and the actuator itself provides the propulsion. A related study was conducted by Kabei et al. who developed electrostatic liner actuators as artificial muscles, which imitate the active sliding between actin and myosin[3)]. However, this sliding is only in a straight direction, and active bending by elastic deformation is not considered.

To realize the propulsion mechanism in water modeled on the active sliding of microtubules of eukaryotic flagella, we are making the enlarged propulsion mechanism in water, which can reproduce the microtubule sliding using electromagnets. This mechanism is not based on micromachines, and could provide a new propulsion mechanism instead of the screw propeller, in particular, for viscous fluids. Furthermore, this mechanism could contribute the basic technical data for the design of micromachines in fluids for future use. We have developed the first model of the propulsion mechanism and measured the thrust force in water[4),(5)]. However, this model could not produce sufficient propulsion force because the magnetic force of the electromagnet was small, and the resulting amplitude was not sufficiently large. In this study, we improved the electromagnet to produce a higher magnetic force and redesigned the propulsion mechanism. This mechanism is capable of changing the bending frequency, the number of waves, and the

* Received 16th May, 2001
** Department of Functional Machinery and Mechanics, Faculty of Textile Science and Technology, Shinshu University, 3-15-1 Tokida, Ueda, Nagano 386-8567, Japan. E-mail: shukoba@giptc.shinshu-u.ac.jp
*** Shinano Kenshi Co. Ltd., 1078 Kami-Maruko, Maruko, Nagano 386-0498, Japan

sliding length corresponding to the amplitude. To determine the performance of this mechanism, we discussed the influence of these parameters on the thrust force.

2. Bending Mechanism and Modeling

2.1 Bending mechanism of flagella[6],[7]

Figure 1 shows a typical structure of a flagellum of sea urchin spermatozoa. The diameter of a single flagellum is about 0.2 μm. Nine outer doublet microtubules and a central pair of singlet microtubules are arranged as shown in the cross section of this figure. Dyneins are located along the microtubules at intervals of 24 nm. A dynein has the force (1 - 4 pN) to move an adjacent microtubule toward the tip of the flagellum. Regions that resist active sliding and passive bending exist in the flagella. During active sliding, microtubules are bent by the configuration of the three regions as shown in Fig. 2. Propagating waves are generated by the movement of each region toward the tip of the flagellum. The bending of flagellum occurs in a plane shown in Fig. 1. If dyneins on the right half (doublets 1 - 5) of the cross section of the axoneme, in particular, the dyneins on doublet 3, are active, active sliding occurs between doublets 3 and 4 and simultaneously, 'passive' sliding occurs between doublets 7 and 8. The bending of flagellum occurs in the direction shown by arrow B. If dyneins on the left half (doublets 6 - 9) of the cross section of the axoneme, in particular, the dyneins on doublet 7, are active, the sliding direction is reversed the and flagellum bends toward the opposite direction (arrow A).

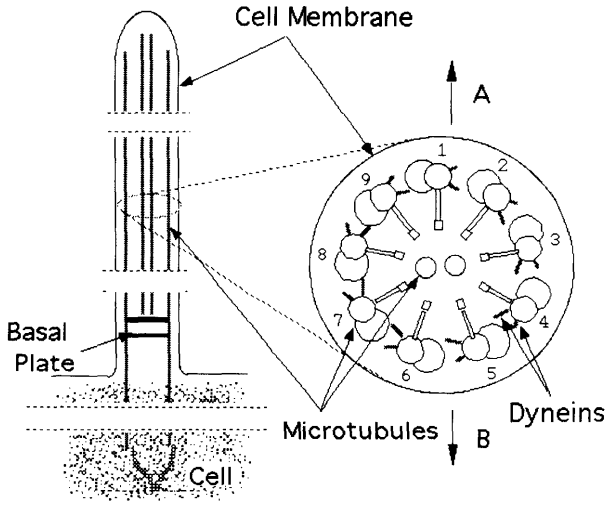

Fig. 1 Typical structure of eukaryotic flagella. The arrows indicate the direction of planar bending

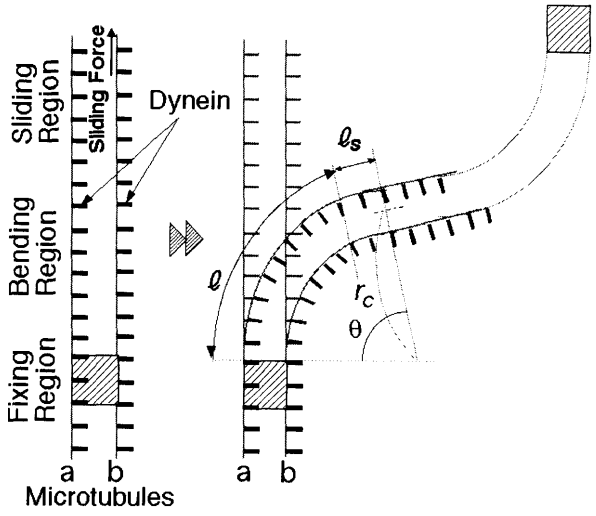

Fig. 2 Bending mechanism of two microtubules

Confusingly, bacterial flagella share the same name as those of eukaryotes, which are not modeled in this study. Their function is entirely different.

2.2 Basic conditions for modeling

To make the propulsion mechanism in water by modeling eukaryotic flagella, the following conditions are fulfilled.

(1) The model consists of two outer microtubules without a central pair of microtubules. This allows the microtubules to produce forces to drive each other, which produces bending in a 2-dimensional plane.

(2) To generate bending, elasticity is given to the model.

(3) Each region is generated at the base corresponding to the joint of the sperm head and the flagellum, and propagated. The basal cell, such as a sperm head, is ignored in the modeling.

(4) The direction of sliding between two microtubules changes alternately. (When the microtubules are represented by a and b, as shown in Fig. 2, first a pushes b, then b pushes a).

3. Propulsion Mechanism in Water

3.1 Configuration

Figure 3 shows the principle of the propulsion mechanism in water using electromagnets to represent 2-dimensional bending by two microtubules. The electromagnets corresponding to dyneins are attached to two flexible beams corresponding to microtubules. The attraction and repulsion forces between the electromagnets generate bending.

The inner structure of the propulsion mechanism in water is shown in Fig. 4, and the photograph is shown in Fig. 5. Thirty electromagnets are arranged on each flexible beam of vinyl chloride at uniform intervals. The sliding length l_s can be changed by changing the distance between adjacent electromagnets D_{em}, shown in Fig. 4. To ensure secure bending,

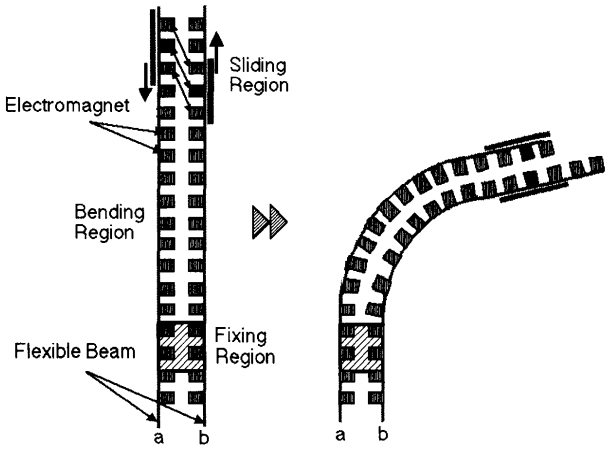

Fig. 3 Bending mechanism of the propulsion mechanism in water

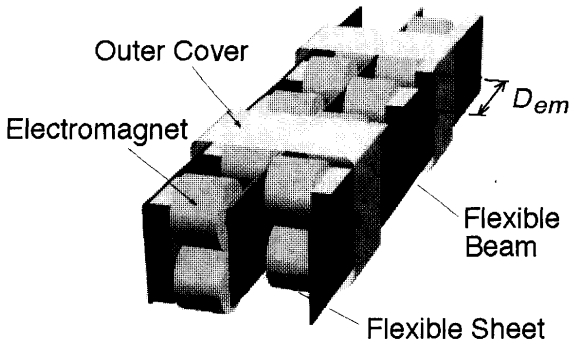

Fig. 4 The structure of the propulsion mechanism in water

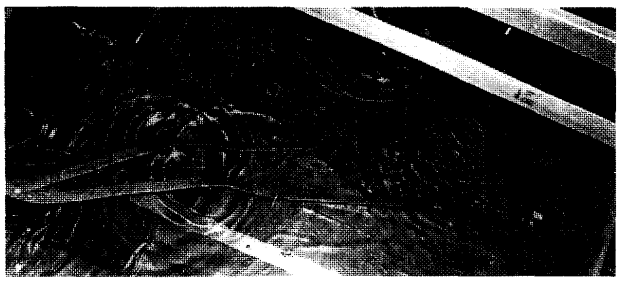

Fig. 5 Photograph of the propulsion mechanism in water

we set the sliding length $l_s = D_{em}/2$. A flexible polytetrafluoroethylene sheet is placed between facing electromagnets to prevent mutual interference. To obtain a rectangular section of the mechanism, several polytetrafluoroethylene outer cover sheets are wound around the mechanism. Figure 6 shows the electromagnet. The iron core is U-shaped and coils are wound on both ends. The iron core is made from electromagnetic soft iron. Enameled copper wire with a diameter of 0.1 mm is used as the coil, and wound with 1 000 turns and a resistance of 23 ohms. We used a modified version of an iron core from the previously used electromagnet[3),4)] to reduce magnetic resistance.

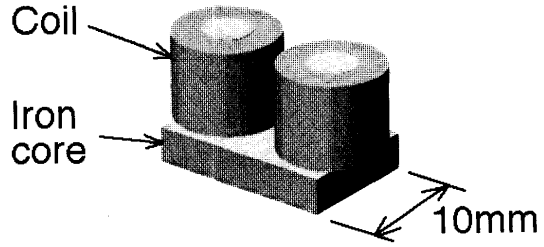

Fig. 6 Electromagnet

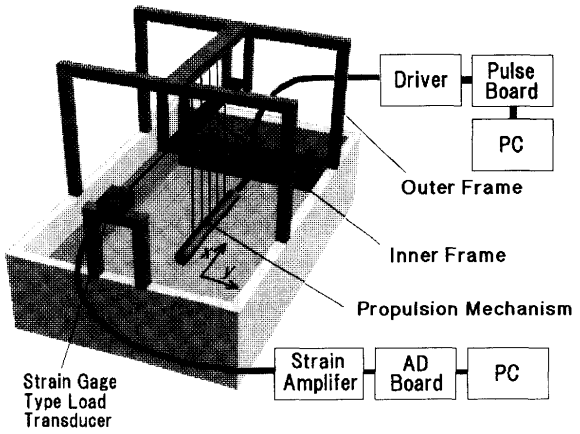

Fig. 7 Experimental system

The iron core of the electromagnet could be a cylindrical shape but we preferred a U-shape to achieve stable bending because no twisting occurs during bending at repulsion. The electromagnets are painted to avoid oxidation of the iron core.

Figure 7 shows the experimental system. Signals are sent from a 128-channel pulse output board (Interface Corp., PCI-2426C) on a personal computer (EPSON Direct Corp., MT-4000) to the driver composed of a relay circuit (Omron Corp., G5V-2-12V). To generate desired bending, the behavior of each electromagnet is calculated in advance and an excitation sequence based on time is prepared as binary data. Based on this, the signals are sequentially output from the pulse board. One bending cycle is divided by an appropriate time interval Δt. Bending frequency is controlled by changing Δt. The propulsion mechanism is hung with nylon string from the inner frame. The length of the nylon string was adjusted at each condition of the experiment to reduce the effect of swinging. Thrust force is detected by the load cell (NEC San-ei Instruments, T1) connected to the inner frame by the nylon string. Initial tension is given to the nylon string between the inner frame and the load cell in order to prevent slackening of the nylon string. The outer frame has guide bars to move the inner frame only in the x direction. To reduce the frictional force between the guide bars and the inner frame, the polytetrafluoroethylene sheets are placed

Table 1 Experimental conditions

Distance between adjacent electromagnets: D_{em}	13 mm - 16 mm
Sliding length: l_s	6.5 mm – 8.0 mm
Total Length of propulsion mechanism: L	530 mm (D_{em} =13mm) - 620 mm (D_{em} =16mm)
Width of propulsion mechanism	23 mm
Height of propulsion mechanism	18 mm
Weight of propulsion mechanism	470 g
Electric current on each electromagnet	1.0 A
Bending frequency: f	0.55 Hz – 0.88 Hz
Number of waves: N_W	1 - 1.5

Table 2 Amplitude A of the bending wave

	l_s =6.5 mm (D_{em} =13 mm)	l_s =7.0 mm (D_{em} =14 mm)	l_s =7.5 mm (D_{em} =15 mm)	l_s =8.0 mm (D_{em} =16 mm)
N_W=1	40 mm	42 mm	46 mm	49 mm
N_W=1.25	35 mm	39 mm	42 mm	45 mm
N_W=1.5	30 mm	35 mm	38 mm	40 mm

between them.

3.2 Experimental conditions

Table 1 lists the experimental conditions. The bending frequency f, the number of waves N_W and the sliding length l_s are changed. The total length of the propulsion mechanism L is also changed by D_{em}. Table 2 lists the values of amplitude A of the bending waves. The value of A is changed by the sliding length l_s for the number of waves N_W.

We defined the Reynolds number Re when the propulsion mechanism is moving in water as,

$$Re=\frac{f\lambda L}{\nu}, \qquad (1)$$

where λ and L are the wavelength and the total length of the mechanism, respectively, and ν is the kinematic viscosity of water at 20 degrees centigrade (1.0×10^{-6} m^2/s). For example, in the case of N_W=1.25, D_{em}=15 mm (λ=320 mm and L=620 mm) and f=1.0 Hz, the Reynolds number is 2.23×10^5 and the inertial force of water surrounding the mechanism is dominant for propulsion. As an example, the value of Re for sea urchin spermatozoa is 2.52×10^{-2} (f, λ, L and ν are approx. 35 Hz, 24 μm and 1.0×10^{-6} m^2/s, respectively)[8]. The resistive force of fluid is dominant for swimming.

4. Results and Discussion

4.1 Bending wave

Figure 8 shows the change in shape of the propulsion mechanism in water (center line only) for the case of 25 divisions in one bending cycle. A wave of A=42 mm and λ=360 mm is propagated from the top to the tail continuously. The thrust force is generated in the x direction.

4.2 Thrust force characteristics

Figure 9 shows the variation of x-directional thrust force F_x for one bending cycle when the thrust force of the propulsion mechanism becomes cyclic. Generally, the thrust force changes twice in one bending cycle. This tendency is similar to that of a multilink propulsion mechanism in water[9], and is explained by the fact that the shapes of the mechanism during the first half and the latter half of one bending cycle are symmetrical with respect to the x-directional centerline of the mechanism. This figure shows the maximum thrust force at 90 and 270 degrees, and the minimum thrust force at 0 and 180 degrees. These phenomena are suggested from the motion of the mechanism shown in Fig. 8 and the slender body theory[10]: The motion of the tail is an important factor for the thrust force in the slender body theory. The motion around the tail consists of swaying and yawing, similar to the motion of a fish's tail. The tail is on the top dead point at 0 degrees of

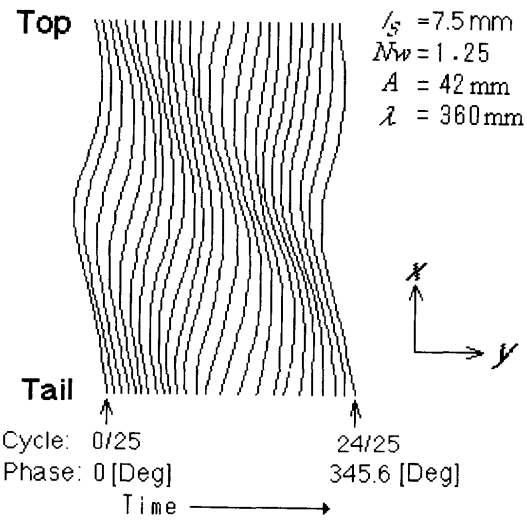

Fig. 8 Bending wave

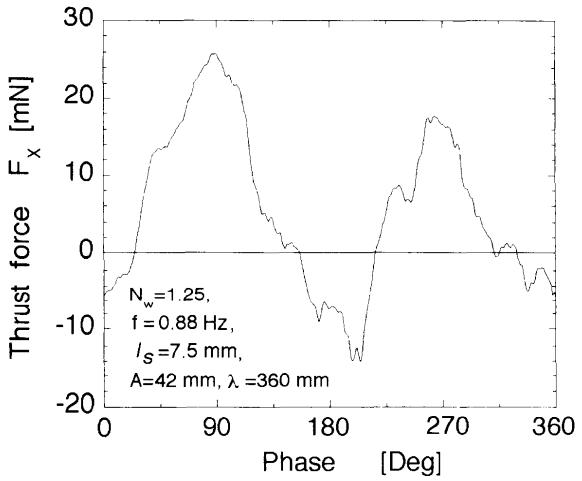

Fig. 9 Variation of x-directional thrust force for one bending cycle

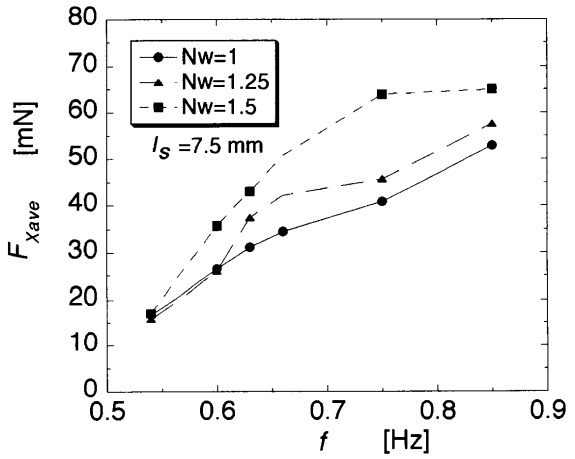

Fig. 10 Relationship between the bending frequency f and average thrust force $F_{x\,ave}$

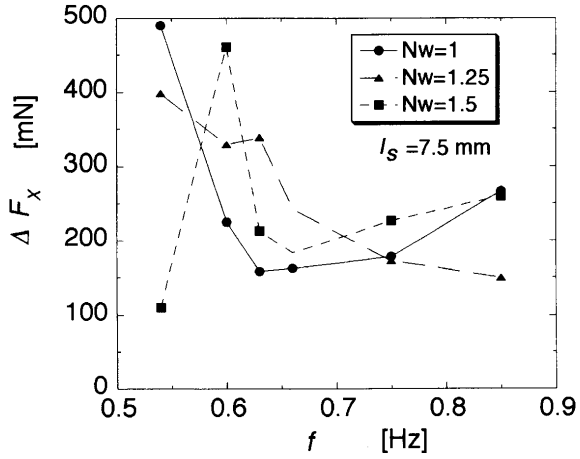

Fig. 11 Relationship between the bending frequency f and the thrust force difference ΔF_x ($=F_{x\,max}-F_{x\,min}$)

phase and on the bottom dead point at 180 degrees of phase. The motions in the middle of phase (around 90 and 270 degrees) generate higher thrust force caused by the reaction force of water. The flow visualization of water surrounding the mechanism and analysis of thrust force are required for further analysis.

Figure 10 shows the relationship between the bending frequency f and the average thrust force $F_{x\,ave}$. The average thrust force $F_{x\,ave}$ increases with an increase in f. It is suggested that the momentum of water is increased with increasing bending wave speed, and acts on the greater thrust force. Furthermore, $F_{x\,ave}$ increases with an increase in N_W. However, in the case of $N_W=1.5$, the rate of increase declines above 0.75 Hz. This is caused by decreased amplitude due to the failure to maintain the desired amplitude: Since the resistance of water increases with increasing bending frequency, the sliding force of the electromagnet and the elastic back force of the flexible beam caused by its bending, become insufficient.

Figure 11 shows the relationship between the bending frequency f and the thrust force difference ΔF_x ($=F_{x\,max}-F_{x\,min}$). ΔF_x is greater for lower f. This can be accounted for by the driving operation of the bending mechanism: Electromagnets are driven by excitation at a time interval Δt, hence, bending of the propulsion mechanism does not show a smooth change and is intermittent. Furthermore, the sliding speed is constant even when the bending frequency is changed. In the case of bending frequency, the intermittence becomes large (in particular, the stoppage time becomes large) with increasing time interval, and as the result the thrust force difference is increased.

Figure 12 shows the relationship between the amplitude A and the average thrust force $F_{x\,ave}$. $F_{x\,ave}$

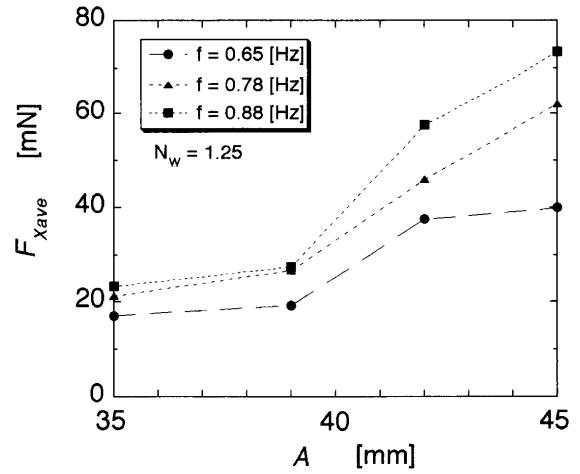

Fig. 12 Relationship between the amplitude A and average thrust force $F_{x\,ave}$

increases with an increase in A. It is suggested that the increased thrust force causes the increased inertial force of water due to the larger amplitude.

Figure 13 shows the relationship between the amplitude A and the thrust force difference ΔF_x ($=F_{x\,max}-F_{x\,min}$). There are no significant influences of A on ΔF_x. However, it is thought that in the case of greater value of A, ΔF_x would be greater due to the increasing change of the inertial force of water and the intermittence. We have to examine the causes from the viewpoint of fluid dynamics and improve the experimental system in the future. Another issue which is required to be addressed in the future includes an experiment for low Reynolds number: When a liquid with a very high kinematic viscosity coefficient is used instead of water, a Reynolds number from previous computer simulations[1),2)] can be used, and it is possible to verify the computer simulation results for thrust force with the law of similarity.

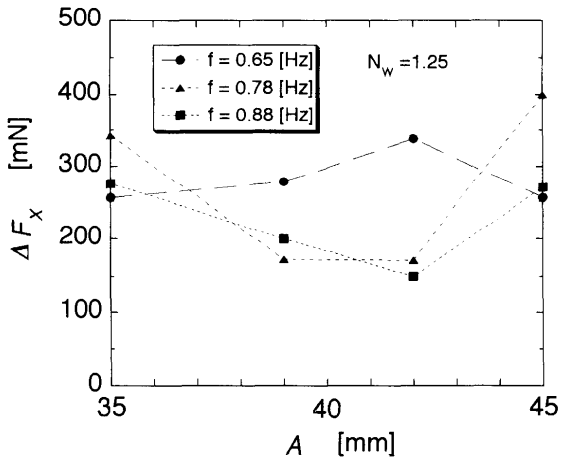

Fig. 13 Relationship between the amplitude A and the thrust force difference ΔF_x ($=F_{x\max}-F_{x\min}$)

This is also applicable to bending mechanisms in fluids with very high viscosity : An example of the Reynolds number of the simulation, $\lambda=32$ μm, $L=64$ μm, $f=1.0$ Hz, and $\nu=1.0\times10^{-6}$ m²/s (the ratio wavelength : total length, frequency and kinematic viscosity are the same as those of the mechanism) is 2.05×10^{-3}. An example of the Reynolds number of the mechanism mentioned in section 3.2 is 2.23×10^{5}. Hence, a value of 109.0 m²/s of ν is required. We require an actuator with higher output power for propulsion in this very highly viscous fluid.

5. Conclusions

This study was conducted to realize an enlarged propulsion mechanism in water modeled on the sliding of microtubules of eukaryotic flagellum. We modified the electromagnet to produce a higher magnetic force, and enabled the choice of sliding length depending on the distance between adjacent electromagnets and the number of waves. We found that the average thrust force of the propulsion mechanism increases with the increase in the amplitude and the number of waves.

Acknowledgements

This work was supported by a research grant from the Research Foundation for the Electrotechnology of Chubu, financial assistance from FANUC FA and Robot Foundation, a Grant-in-Aids for Scientific Research (13450096-01, 13650275-00) by the Japan Society for the Promotion of Science and a Grant-in-Aids for COE Research (10CE2003) by the Ministry of Education, Culture, Sports, Science and Technology of Japan.

References

(1) Kobayashi, S., Shibasaki, Y. and Morikawa, H., Simulation Study for Micropropulsion Mechanism in Liquid Modeled on Sliding Mechanism of Microtubules in Flagella, JSME Int. J., Ser. C, Vol. 42, No. 3 (1999), pp. 730-736.

(2) Kobayashi, S., Takizawa, O. and Morikawa, H., Simulation Study of Elastic Micropropulsion Mechanism Modeled on Sliding Mechanism of Microtubules in Flagella in Liquid, JSME Int. J., Ser. C, Vol. 43, No. 4 (2000), pp. 845-852.

(3) Kabei, N., Murayama, T., Nagayake, K. and Tsuchiya, K., Electrostatic Liner Actuators Developed as Biomimicking Skeletal Muscle, Trans. Jpn. Soc. Mech. Eng., (in Japanese), Vol. 60, No. 578, C(1994), pp. 3392-3397.

(4) Kobayashi, S., Furihata, K., Takizawa, O. and Morikawa, H., Propulsion Mechanism Modeled on Microtubule Sliding of Eukaryotic Flagella, Proc. of 1st Int. Conf. on Aqua Bio-Mechanisms, (2000), pp. 93-98.

(5) Kobayashi, S., Furihata, K. and Morikawa, H., Propulsion Mechanism Modeled on Bending Mechanism of Eukaryotic Flagellar Bending in Water, J. of Robotics and Mechatoronics, Vol. 13, No. 1 (2001), pp. 96-100.

(6) Zoological Society of Japan, Cell Motility, (in Japanese), (1974), Tokyo Daigaku Shuppankai.

(7) Murase, M., The Dynamics of Cellular Motility, (1992), pp. 102-111, John Wiley & Sons.

(8) Gray, J. and Hancock, G.J., The Propulsion of Sea-Urchin Spermatozoa, J. Exp. Biol., Vol. 32 (1955), pp. 802-814.

(9) Kobayashi, S., Propulsion Force Characteristics of Propulsion Mechanism Imitating Bending-movement Organisms in Water, Trans. Jpn. Soc. Mech. Eng., (in Japanese), Vol. 60, No. 579, B (1994), pp. 3613-3617.

(10) Lighthill, M.J., Note on the Swimming of Slender Fish, J. Fluid Mech., Vol. 9 (1960), pp. 305-317.